

RESEARCH ARTICLE

Thermal acclimation of photosynthetic activity and RuBisCO content in two hybrid poplar clones

Lahcen Benomar^{1*}, Mohamed Taha Moutaoufik², Raed Elferjani³, Nathalie Isabel⁴, Annie DesRochers⁵, Ahmed El Guellab¹, Rim Khelifa⁶, Lala Amina Idrissi Hassania⁷

1 Faculté de foresterie, de géographie et de géomatique, Université Laval, Québec, QC, Canada, **2** Department of Biochemistry, University of Regina, Regina, SK, Canada, **3** Saskatoon Research and Development Centre, Agriculture and Agri-Food Canada, Saskatoon, SK, Canada, **4** Natural Resources Canada, Canadian Forest Service, Laurentian Forestry Centre, Québec, QC, Canada, **5** Université du Québec en Abitibi-Témiscamingue, Amos, QC Canada, **6** Département des sciences biologiques, Université du Québec à Montréal, Montréal, QC, Canada, **7** Laboratoire de Biotechnologies végétales, É, Faculté des Sciences, Université Ibn Zohr Agadir, Morocco

* lahcen.benomar.1@gmail.com



OPEN ACCESS

Citation: Benomar L, Moutaoufik MT, Elferjani R, Isabel N, DesRochers A, El Guellab A, et al. (2019) Thermal acclimation of photosynthetic activity and RuBisCO content in two hybrid poplar clones. PLoS ONE 14(2): e0206021. <https://doi.org/10.1371/journal.pone.0206021>

Editor: Janusz J. Zwiazek, University of Alberta, CANADA

Received: October 1, 2018

Accepted: January 25, 2019

Published: February 11, 2019

Copyright: © 2019 Benomar et al. This is an open access article distributed under the terms of the [Creative Commons Attribution License](https://creativecommons.org/licenses/by/4.0/), which permits unrestricted use, distribution, and reproduction in any medium, provided the original author and source are credited.

Data Availability Statement: all relevant data are within the manuscript and its Supporting Information files.

Funding: This research was funded by Genomics R&D Initiative (<http://grdi-irdg.collaboration.gc.ca/eng/>) grants to NI (Natural Resources Canada) and NSERC discovery Grant (http://www.nserc-crsng.gc.ca/ResearchPortal-PortailDeRecherche/Instructions-Instructions/DG-SD_eng.asp) to AD. The funders had no role in study design, data

Abstract

The mechanistic bases of thermal acclimation of net photosynthetic rate (A_n) are still difficult to discern, and the data sets available are scarce, particularly for hybrid poplar. In the present study, we examined the contribution of a number of biochemical and biophysical traits on thermal acclimation of A_n for two hybrid poplar clones. We grew cuttings of *Populus maximowiczii* × *Populus nigra* (M×N) and *Populus maximowiczii* × *Populus balsamifera* (M×B) clones under two day/night temperature of 23°C/18°C and 33°C/27°C and under low and high soil nitrogen level. After ten weeks, we measured leaf RuBisCO (RAR) and RuBisCO activase ($RARCA$) amounts and the temperature response of A_n , dark respiration (R_d), stomatal conductance, (g_s), apparent maximum carboxylation rate of CO₂ (V_{cmax}) and apparent photosynthetic electron transport rate (J). Results showed that a 10°C increase in growth temperature resulted in a shift in thermal optimum (T_{opt}) of A_n of 6.2±1.6°C and 8.0±1.2°C for clone M×B and M×N respectively, and an increased A_n and g_s at the growth temperature for clone M×B but not M×N. RuBisCO amount was increased by N level but was insensitive to growth temperature while $RARCA$ amount and the ratio of its short to long isoform was stimulated by the warm condition for clone M×N and at low N for clone M×B. The activation energy of apparent V_{cmax} and apparent J decreased under the warm condition for clone M×B and remained unchanged for clone M×N. Our study demonstrated the involvement of both $RARCA$, the activation energy of apparent V_{cmax} and stomatal conductance in thermal acclimation of A_n .

collection and analysis, decision to publish, or preparation of the manuscript.

Competing interests: The authors have declared that no competing interests exist.

Introduction

Global warming may lead to a significant reduction of forest productivity through a decrease in net assimilation rate of CO₂ [1, 2]. Plant physiological processes including photosynthetic rate (A_n) and dark respiration (R_d) are strongly temperature-dependent, and their acclimation may help trees maintain a normal growth when temperature shifts from optimum to warm [2–4]. Thermal acclimation of A_n is achieved through adjustments of morphological, biochemical and biophysical components of photosynthesis which may occur via (i) a shift of the thermal optimum of A_n (T_{opt}) toward the new growth temperature (Fig 1) (ii) an increase or a maintenance of the photosynthetic rate at T_{opt} ($A_{n_{opt}}$) at warmer growth temperatures (iii) a shift in both $A_{n_{opt}}$ and T_{opt} . These shifts would result in an increase or maintenance of the photosynthetic rate respective to growth temperature ($A_{n_{growth}}$) [5–7]. The mechanisms involved in thermal acclimation of photosynthesis are still difficult to discern and may differ among populations or species from sites with different temperature regimes [8].

Photosynthetic processes that might be subject to acclimation include (i) the reference values (at 25°C) of maximum carboxylation rate (V_{cmax}^{25}) and maximum electron transport rate (J_{max}^{25}), (ii) the temperature response of both V_{cmax} and J_{max} (activation and deactivation energy) and (iii) the temperature response of stomatal and mesophyll conductance [5–7, 9].

Leaf nitrogen (N) might be a limiting factor of carbon assimilation processes and hence plant growth and survival [10, 11], as most of the leaf nitrogen is allocated to proteins involved in light harvesting, Calvin-Benson cycle and electron transfer along thylakoid membranes [12, 13]. Leaf nitrogen content is generally deficient in temperate and boreal regions and has been shown to decrease in response to increasing growth temperature [14–16]. A decrease in leaf N in response to increasing growth temperature may result in a decrease of RuBisCO content [16]. This has been proposed as an explanation of the commonly observed decrease in V_{cmax} at temperatures above the optimum and the resulting lack of thermal acclimation of A_n [16, 17]. On the other hand, Yamori et al.'s [18] found that photosynthesis temperature response of several C₃ plants was generally RuBP carboxylation-limited above the T_{opt} at low leaf nitrogen content while, under high N level, it shifted to a limitation by RuBP regeneration. However, the effect of temperature on the limiting steps of A_n (V_{cmax} vs. J_{max}) may depend on the response of CO₂ conductance (g_s and g_m) as well [19–22]. Moreover, RuBisCO-related effect on A_n at above-optimal temperature may depend on the plasticity of J_{max}^{25} to V_{cmax}^{25} ratio. From this perspective, this may be applicable only for cold-adapted plant species, which are

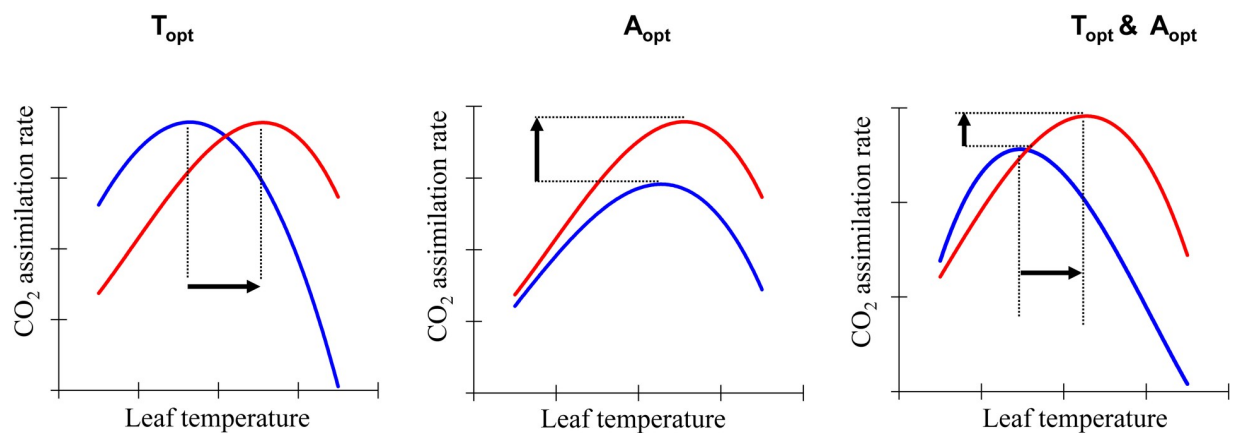


Fig 1. Illustration of scenarios of thermal acclimation of photosynthetic rate. Adapted from Way and Yamori [6]. Blue and red curves indicate the growth under cool and warmer temperature, respectively.

<https://doi.org/10.1371/journal.pone.0206021.g001>

characterized by a higher J_{\max}^{25} to V_{\max}^{25} ratio and low or lack of its adjustment in response to both N level and growth temperature [19, 23]. Weston et al.'s [24] did not observe any change in RuBisCO concentration for two genotypes of *Acer rubrum* grown under hot and optimal temperatures. Then, more research is needed to unravel the multiple factors involved in the response of carbon assimilation to above-optimal temperatures. In fact, it has been proven that V_{\max} does not only depend on RuBisCO concentration but also on its activation state (inhibited/activated) [2, 25, 26]. The activation state of RuBisCO is regulated by the RuBisCO activase, a heat-labile enzyme using energy via ATP hydrolysis to release inhibitors from the active site of RuBisCO [26–28]. A decrease in RuBisCO activase activity has been documented as a primary cause of reducing RuBisCO activity and then photosynthetic performance in response to increasing growth temperature [26, 28, 29]. RuBisCO activase is a stromal protein existing in two isoforms of 41–43 kDa (short isoform) and 45–46 kDa (long isoform) that arise from one single gene with an alternatively spliced transcript or from two separate genes. Still, the specific physiological role of a given isoform with respect to heat stress is generally not understood. Recent studies from herbaceous species demonstrated an increase in the two RuBisCO activase forms or a shift in the balance between them when plants were exposed to temperature above 30°C [7, 24, 30–32].

Here we used *Populus*, a model tree in forestry to study the physiological thermal acclimation because of its commercial and environmental importance in the northern hemisphere and its fast growth rate. Information on the response of photosynthesis to higher temperature for tree species is limited in general, and previous studies conducted on *Populus balsamifera* [33], *Populus tremuloides* [34], *Populus nigra* [35], *Populus grandidentata* [15] and *Populus deltoides* × *nigra* [36] found little evidence of a thermal acclimation of A_n to increasing temperatures. Nevertheless, little research focused on the physiological and molecular mechanisms underlying the observed thermal acclimation of trees. The objective of the present study was to examine to what extent leaf nitrogen, RuBisCO and RuBisCO activase content are involved in thermal acclimation of photosynthetic activity in hybrid poplars. We tested two hypotheses: (1) Leaf N and RuBisCO amounts *per se* are not involved in thermal acclimation of A_n . (2) The increase of the RuBisCO activase and or differential expression of its isoforms under warm conditions contribute to thermal acclimation of A_n .

Methodology

Plant material and growth conditions

This experiment was conducted in greenhouses and growth chambers at Université Laval, Québec, Canada, from January to May 2017. Dormant cuttings of two hybrid poplar clones: M×N (*Populus maximowiczii* × *Populus nigra*) and M×B (*Populus maximowiczii* × *Populus balsamifera*) were provided by the Québec's Ministère des Forêts, de la Faune et des Parcs (MFFP) from the forest nursery of Berthier (Berthierville, Québec, Canada) during early January after chilling needs were met. These clones were recommended by MFFP for the south of Quebec. Cuttings were planted in 2 L pots filled with peat/vermiculite substrate ($v/v = 3/1$) and placed in two greenhouses where day/night temperatures were 23°C/18°C and 33°C/27°C. Plants were grown under a Photosynthetically-active Photon Flux Density (PPFD) ranging between 400 and 700 $\mu\text{mol m}^{-2} \text{s}^{-1}$, a relative humidity of 65% and a 8/16 h dark/light photoperiod using 400 W metal halide lamps. Cuttings were irrigated daily to maintain full soil field capacity. After four weeks, for better control of growth conditions (mainly temperature and relative humidity), pots were transferred to growth chambers (model PGW 36, Conviron, Winnipeg, Canada) under a split-split-plot layout; the Temperature × Clone as the first split and Nitrogen level as the second split. The same environmental parameters as in greenhouses

were used, except for PPFD which was kept at a constant rate of $500 \mu\text{mol m}^{-2} \text{s}^{-1}$ during day time. In each growth chamber, half of the plants ($n = 18$) were randomly assigned to receive a low-nitrogen fertilization treatment (5 mM, LN) while the other half received a high-nitrogen (20 mM, HN). Nitrogen was added, every week, using (20N-20P-20K) fertilizer dissolved in distilled water. Plants ($n = 72$; 2 growth temperatures \times 2 nitrogen levels \times 2 hybrid poplar clones \times 9 replicates) were allowed to acclimate to respective growth conditions for six weeks before measurements were taken. Pots were moved within each chamber every third day to eliminate any position-related bias.

Gas exchange measurements

After ten weeks of growth, leaf-level gas exchange was measured on the 4th fully expanded leaf from the top of each plant using two cross-calibrated portable open-path gas-exchange systems (Li-6400, Li-Cor Inc., Lincoln NE), equipped with a 2×3 cm broadleaf chamber (Li-6400-40, Li-Cor Inc). The measurements were made on 24 plants in total (3 replicates \times 2 clones \times 2 temperatures \times 2 N levels). Given the limited control capacity of LI-6400 system on leaf temperature in the cuvette (T_{leaf} can be set to $\pm 6^\circ\text{C}$ of the ambient temperature), measurements were performed in a growth chamber under controlled temperature and relative humidity. Growth chamber temperature was set manually to desired T_{leaf} allowing an effective and quick easy adjustment over the $10\text{--}40^\circ\text{C}$ range and an exposure of the whole plant to the targeted temperature.

The temperature was increased from 10°C to 40°C with 5°C increment and plants were allowed to acclimate for at least 20 min to each step. At each temperature, we measured dark respiration (R_d) followed by $A-C_i$ response curve records with a 10-minutes period between R_d and $A-C_i$ respected to allow complete opening of stomata. $A-C_i$ response curves were recorded at each temperature after at least 10 min of steady state at ambient CO_2 partial pressure $C_a = 400 \mu\text{mol mol}^{-1}$ and a saturating $PPFD = 800 \mu\text{mol m}^{-2} \text{s}^{-1}$. The saturated $PPFD$ was determined from measured $A-Q$ curve on 3 plants from each Clone \times Growth T° combination at 25°C . Thereafter, the reference CO_2 (C_a) was changed in the following order: 400, 350, 300, 200, 100, 50, 400, 500, 600, 800, 900, 1000, 1200, 1400, and $1600 \mu\text{mol mol}^{-1}$. Values were recorded based on the stability of photosynthesis, stomatal conductance (g_s), CO_2 and water vapour concentration. The vapour pressure difference (VPD) during measurement varied from 0.5 to 3.2 KPa from low to high temperature. At high temperature, the VPD was lowered as much as possible by maintaining the relative humidity (RH) at 70% inside the growth chamber. At low temperature, RH was maintained at 50% to maintain VPD as high as 0.5 KPa. For each sample, data required were collected generally within one or two days (10–14 h). The list of abbreviations and symbols are given in Table 1.

Estimation of gas exchange variables

The photosynthetic capacity variables, V_{cmax} and J_{max} , were estimated from gas-exchange by fitting the $A-C_i$ curve with the biochemical model of C_3 [37], assuming infinite mesophyll conductance (g_m). In fact, the estimation of g_m from $A-C_i$ is very challenging as it depends on the number of data points on the $A-C_i$ curve and goodness-of-fit of the curve which is difficult to achieve at high and low temperatures. In this experiment, we tried to estimate g_m from $A-C_i$ curves following Ethier et al.'s [38] and Miao et al.'s [39] without success as about 45% of them gave non-meaningful estimates.

The model was thus fitted using non-linear regression techniques (Proc NLIN, SAS) following Dubois et al.'s [40]. Briefly, the net assimilation rate (A_n) is given as:

$$A_n = \min\{A_c, A_j\} \quad (1)$$

Table 1. List of abbreviations.

Symbol	Definition	Unit
A_c	RuBP-saturated CO ₂ assimilation rate	$\mu\text{mol CO}_2 \text{ m}^{-2} \text{ s}^{-1}$
$A_{n\text{-growth}}$	Photosynthetic rate at growth temperature	$\mu\text{mol CO}_2 \text{ m}^{-2} \text{ s}^{-1}$
A_n	Net CO ₂ assimilation rate	$\mu\text{mol CO}_2 \text{ m}^{-2} \text{ s}^{-1}$
A_j	RuBP-limited CO ₂ assimilation rate	$\mu\text{mol CO}_2 \text{ m}^{-2} \text{ s}^{-1}$
$A_{n\text{-opt}}$	Photosynthetic rate at T_{opt}	$\mu\text{mol CO}_2 \text{ m}^{-2} \text{ s}^{-1}$
C_a	Atmospheric CO ₂ concentration	$\mu\text{mol mol}^{-1}$
C_i	intercellular CO ₂ concentration	$\mu\text{mol mol}^{-1}$
E_a	Activation energy	KJ mol^{-1}
E_d	Energy of deactivation	KJ mol^{-1}
g_s	Stomatal conductance	$\text{mol H}_2\text{O m}^{-2} \text{ s}^{-1}$
J	Electron transport rate	$\mu\text{mol e}^- \text{ m}^{-2} \text{ s}^{-1}$
J_{max}^{25}	Maximal electron transport rate at leaf temperature of 25°C	$\mu\text{mol e}^- \text{ m}^{-2} \text{ s}^{-1}$
$J_{max}^{25}:V_{cmax}^{25}$	Ratio of maximal electron transport to maximal carboxylation rate at leaf temperature of 25°C	
N_{area}	Leaf nitrogen in area basis	g m^{-2}
O	Partial atmospheric pressure of O ₂	mmol mol^{-1}
PPFD	Photosynthetically-active Photon Flux Density	$\mu\text{mol m}^{-2} \text{ s}^{-1}$
SLA	Specific leaf area	$\text{cm}^2 \text{ g}^{-1}$
R_{day}	Non-photorespiratory mitochondrial respiration in the light	$\mu\text{mol CO}_2 \text{ m}^{-2} \text{ s}^{-1}$
R_d	Dark respiration	$\mu\text{mol CO}_2 \text{ m}^{-2} \text{ s}^{-1}$
R_d^{10}	R_d at leaf temperature of 10°C	$\mu\text{mol CO}_2 \text{ m}^{-2} \text{ s}^{-1}$
T_{opt}	Thermal optimum	°C
K_c	Michaelis–Menten constants of RuBisCO for CO ₂	$\mu\text{mol mol}^{-1}$
K_o	Michaelis–Menten constants of RuBisCO for O ₂	mmol mol^{-1}
Q_{10}	Rate of change in R_d with a 10°C increase in temperature	
Γ^*	CO ₂ compensation point in the absence of mitochondrial respiration	$\mu\text{mol mol}^{-1}$
A	Efficiency of light energy conversion	
V_{cmax}	Maximal carboxylation rate	$\mu\text{mol CO}_2 \text{ m}^{-2} \text{ s}^{-1}$
V_{cmax}^{25}	Maximal carboxylation rate at leaf temperature of 25°C	$\mu\text{mol CO}_2 \text{ m}^{-2} \text{ s}^{-1}$

<https://doi.org/10.1371/journal.pone.0206021.t001>

$$A_c = V_{cmax} \frac{(C_i - \Gamma^*)}{C_i + K_c(1 + O/K_o)} - R_{day} \quad (2)$$

$$A_j = J \frac{C_i - \Gamma^*}{4(C_i + 2\Gamma^*)} - R_{day} \quad (3)$$

$$J = \frac{\alpha Q}{\sqrt{1 + \left(\frac{\alpha Q}{J_{max}}\right)^2}} \quad (4)$$

where V_{cmax} is the apparent maximum rate of carboxylation ($\mu\text{mol CO}_2 \text{ m}^{-2} \text{ s}^{-1}$), O is the partial atmospheric pressure of O₂ (mmol mol^{-1}), Γ^* is the CO₂ photo-compensation point in the absence of mitochondrial respiration, R_{day} , is mitochondrial respiration in the light ($\mu\text{mol CO}_2 \text{ m}^{-2} \text{ s}^{-1}$), C_i is the intercellular (substomatal) concentration of CO₂ ($\mu\text{mol mol}^{-1}$), K_c ($\mu\text{mol mol}^{-1}$) and K_o (mmol mol^{-1}) are the Michaelis–Menten constants of RuBisCO for CO₂ and O₂, respectively, J is the apparent rate of electron transport ($\mu\text{mol e}^- \text{ m}^{-2} \text{ s}^{-1}$), J_{max} is the apparent maximum rate of electron transport ($\mu\text{mol e}^- \text{ m}^{-2} \text{ s}^{-1}$), Q is the incident PPFD ($\mu\text{mol m}^{-2} \text{ s}^{-1}$), α is the efficiency of light energy conversion (0.18) which represents

the initial slope of the photosynthetic light response curve [39]. The values at 25°C used for K_c , K_o and I^* were 272 $\mu\text{mol mol}^{-1}$, 166 mmol mol^{-1} and 37.4 $\mu\text{mol mol}^{-1}$, respectively and their temperature dependency was from Bernacchi *et al.*'s [41]. Most of the $A-C_i$ curves at 35°C and 40°C measured for low nitrogen level at 23°C failed to converge and estimates of apparent V_{cmax} and apparent J could not be obtained.

Characterization of the temperature responses of gas exchange variables

Photosynthesis temperature response curves were fitted individually with a quadratic model following Battaglia *et al.*'s [42]:

$$A_n(T) = A_{opt} - b(T - T_{opt})^2 \tag{5}$$

where $A_n(T)$ is the photosynthetic rate at temperature T in °C, $A_{n_{opt}}$ is the photosynthetic rate at the temperature optimum (T_{opt}), and the parameter b describes the spread of the parabola.

$A_{n_{growth}}$ was then estimated using the obtained parameters from Eq (5) for each curve. The daytime temperature was used as growth temperature given the uncertainty regarding the effect of nighttime temperature on A_n .

Dark respiration temperature response curves were fitted with a model in Eq (6) to estimate the Q_{10} (the change in respiration with a 10°C increase in temperature) following Atkin *et al.*'s [3]:

$$R_d(T) = R_d^{10} Q_{10}^{[(T-10)/10]} \tag{6}$$

where R_d^{10} is the measured basal rate of R_d at the reference temperature of 10°C.

The responses of apparent V_{cmax} and apparent J to leaf temperature were fitted using the following two models (Eqs (7) and (8)) depending on the presence or not of deactivation above thermal optimum following Medlyn *et al.*'s [4]:

$$f(T_k) = e^{(c - \frac{E_a}{RT})} \tag{7}$$

$$f(T_k) = k_{opt} \frac{E_d \exp\left[\frac{E_a(T_k - T_{opt})}{T_k R T_{opt}}\right]}{E_d - E_a \left[1 - \exp\left(\frac{E_d(T_k - T_{opt})}{T_k R T_{opt}}\right)\right]} \tag{8}$$

where E_a is the activation energy, E_d is the energy of deactivation, K_{opt} is the apparent V_{cmax} or apparent J at the temperature optimum (T_{opt}). E_d was fixed at 200 KJ mol^{-1} [4] to reduce the number of estimated parameters to three.

Specific leaf area and leaf nitrogen

Leaves used for gas exchange measurements were collected and immediately placed in dry ice before being stored at -20°C and processed within a week for protein extraction. The extracts were kept at -80°C and dosage of proteins (RuBisCO and RuBisCO activase) was done once all samples were extracted. Symmetric leaves (by the stem) were also collected to measure projected area with WinSeedle (Version 2007 Pro, Regent Instruments, Québec, Canada). Samples were then oven-dried for 72h at 56°C, and their dry mass determined. Specific leaf area (SLA) was calculated as the ratio of the projected leaf area (cm^2) to the leaf dry mass (g). Later, leaves were ground separately and N content determined at Université Laval using a LECO elemental analyzer (LECO Corporation, St Joseph, MI, USA).

Extraction and dosage of RuBisCO and RuBisCO activase

Proteins were extracted from frozen leaves at -20°C within less than one week after leaf harvesting following the method outlined in Yamori and von Caemmerer [28]. Briefly, 100 mg of leaves were initially ground in liquid nitrogen using a mortar and pestle. Proteins were extracted on ice using a protein extraction buffer containing 50 mM HEPES-KOH pH 7.8, 10 mM MgCl_2 , 1 mM EDTA, 5 mM DTT, 0.1% Triton X100 (v/v) and protease inhibitor cocktail (Roche). The extracts were kept at -80°C , and once all samples were extracted, the solutions were centrifuged at 16,000g for 1 min followed by determination of the concentration of total soluble proteins (TSP) in the supernatant by the Bradford method [43].

After dosage, 4 \times sample buffer (250 mM Tris-HCl, pH 6.8, 40% glycerol, 8% SDS, 0.2% Bromophenol-blue, 200 mM DTT) was added to proteins extracts, heated at 100°C for 5 min and then centrifuged at 16,000 g for 5 min. After cooling to room temperature, a volume representing 20 μg of total TSP extract of each sample was loaded onto 12% SDS-polyacrylamide gel electrophoresis (SDS-PAGE). The electrophoresis was carried out at room temperature at a constant voltage (120 V). Following SDS-Page, the proteins were transferred to a nitrocellulose membrane (Life Sciences, Mississauga, Canada) for western blot.

Blots were incubated with 5% non-fat milk in TBST (50 mM Tris, pH 7.5, 150 mM NaCl, 0.1% Tween-20) for 60 min, the membranes were washed twice with TBST and incubated with antibodies against RuBisCO (Agriser AB, Vännäs, Sweden) or RuBisCO activase (Agriser AB, Vännäs, Sweden) at room temperature for 60 min. Membranes were washed three times with TBST for 10 min and incubated with secondary antibodies peroxidase-conjugated (Goat Anti-Chicken (Abcam) for RuBisCO and Goat Anti-Rabbit (Abcam) for RuBisCO activase) during 60 min at room temperature. Blots were washed with TBST three times and developed with the ECL system using Odyssey Infrared Imaging System (Li-COR, Biosciences). Images were analyzed using ImageJ [44] to determine the band densities of each sample. The RuBisCO, RuBisCO activase and its two isoforms concentration were expressed as relative to the sample representing the highest density (RAR and RARCA respectively) [31, 45, 46].

Statistical analysis

Three-way analysis of variance was performed to test the effect of growth temperature, clone and nitrogen level on response variables using MIXED procedure of SAS (SAS Institute, software version 9.4, Cary, NC, USA). We used Proc Glimmix for response variables (apparent V_{cmax}^{25} , apparent J_{max}^{25} and E_a) which did not meet the assumptions of residual normality and homoscedasticity even with transformations. Means were compared by the adjusted Tukey method and differences were considered significant if $P \leq 0.05$.

Results

Temperature response of A_n and R_d

The temperature response curves of net photosynthesis under saturating irradiance (A_n) were nicely fitted with a parabolic function (Fig 2A and 2B). Thermal optima (T_{opt}) of A_n differed between clones and increased in response to growth temperature. Low nitrogen level constrained the adjustment of T_{opt} for clone M \times N but not M \times B (Table 2). Also, T_{opt} was below growth temperature except for clone M \times B at 23°C . The two hybrid poplar clones showed different trends regarding A_n at T_{opt} (A_{n_opt}) which increased with increasing growth temperature for clone M \times B and remained unaffected for clone M \times N under high N treatment. A_{n_growth} had a similar trend as A_{n_opt} in response to growth temperature and N level. Both A_{n_growth} and A_{n_opt} declined at low N level for both clones (Table 2).

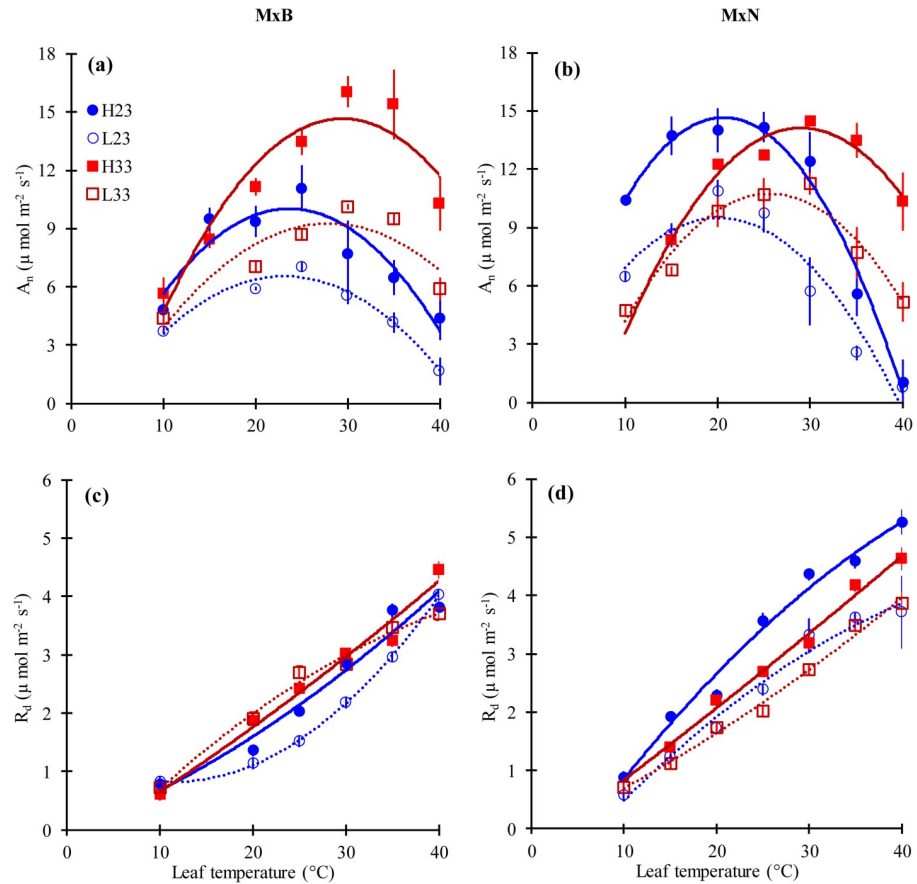


Fig 2. The response of net photosynthesis (A_n) and dark respiration (R_d) to leaf temperature for hybrid poplar clone MxB (a, c) and clone MxN (b, d) grown under two temperatures and two nitrogen levels. H23 and L23 are treatments of high and low nitrogen level respectively at an ambient day temperature of 23°C; H33 and L33 are treatments of high and low nitrogen level at 33°C ambient day temperature. Data are represented by means \pm SE ($n = 3$). P value and R^2 of curves are given in S2 Table.

<https://doi.org/10.1371/journal.pone.0206021.g002>

The two hybrid poplar clones had a different thermal response of dark respiration (R_d) (Fig 2C and 2D). The rate of R_d (R_d^{25}) decreased by augmenting growth temperature for clone MxN at high N level and increased by augmenting growth temperature for clone MxB at low N level (Table 2). Q_{10} decreased when growth temperature was increased, irrespective of N level for clone MxN. In contrast, Q_{10} of clone MxB increased in response to growth temperature raise when N level was high and unchanged at low N level (Table 2).

Temperature response of apparent V_{cmax} and J

Apparent V_{cmax}^{25} was insensitive to growth temperature at low N level for both clones. In contrast, at high N level, apparent V_{cmax}^{25} increased for clone MxB and decreased for clone MxN when growth temperature was increased (Fig 3). Apparent J_{max}^{25} decreased with increasing growth temperature for plants growing at high N level and was insensitive to growth temperature at low N level (Fig 3). The ratio apparent J_{max}^{25} : apparent V_{cmax}^{25} decreased with increasing growth temperature at high N level for clone MxB but not for clone MxN (Table 2). At low N level, apparent J_{max}^{25} : apparent V_{cmax}^{25} ratio was insensitive to growth temperature.

The temperature response curves of apparent V_{cmax} and apparent J were affected by growth temperature but not by nitrogen level. In fact, at the cooler growth temperature, apparent

Table 2. Means (\pm SE) of thermal acclimation-related traits of two hybrid poplar clones (MxB and MxN) grown at day/night temperature of 23/18°C and 33/27°C under high (HN) and low (LN) nitrogen levels (n = 3).

	Clone MxB				Clone MxN			
	23°C		33°C		23°C		33°C	
	HN	LN	HN	LN	HN	LN	HN	LN
$T_{opt}(A_n)$	23.1 (1.2)bc	24.1 (1.2)b	30.3 (1.3)a	29.3 (1.3)a	20.5 (1.2)c	19.7 (1.3)c	30.1 (1.3)a	26.1 (1.3)b
A_{n_opt}	10.1 (0.8)b	7.1(0.8)d	14.9 (0.8)a	9.3 (0.8)cb	15.1 (0.8)a	9.1 (0.8)c	14.2 (0.8)a	10.9 (0.8)b
A_{n_growth}	10.6(1.0)b	6.9(0.9)c	13.9(1.1)a	8.9(1.1)c	14.9(1.1)a	9.6(0.9)c	13.4(1.1)a	9.5(1.1)c
R_d^{25}	2.02(0.2)c	1.51(0.2)d	2.41(0.2)bc	2.61(0.2)b	3.56(0.2)a	2.39(0.2)bc	2.66(0.2)b	2.01(0.2)c
$Q_{10}(R_d)$	1.9(0.1)b	1.8(0.1)b	2.0(0.1)a	1.9(0.1)b	2.0(0.1)a	2.2(0.1)a	1.8(0.1)b	1.8(0.1)b
g_{s_growth}	0.16(0.01)c	0.17(0.01)bc	0.26(0.01)a	0.20(0.01)b	0.20(0.01)b	0.16(0.01)c	0.18(0.01)bc	0.13(0.01)d
$T_{opt}(\text{apparent } V_{cmax})$	33(1.5)	-	NA	NA	34(1.2)	-	NA	NA
$E_a(\text{apparent } V_{cmax})$	75 (3)a	-	49(3)b	57(3)b	58(3)b	-	54(3)b	55(3)b
$T_{opt}(\text{apparent } J)$	34 (1.9)	-	NA	NA	30(1.1)	-	NA	NA
$E_a(\text{apparent } J)$	46(2)a	-	32(2)b	28(2)b	34(2)ab	-	28(2)b	33(2)b
apparent J_{max}^{25} : apparent V_{cmax}^{25}	2.43(0.1)ab	1.68(0.15)c	1.53(0.15)c	1.81(0.19)bc	2.68(0.15)a	2.01 (0.15)bc	2.42(0.19)ab	1.95(0.16)b
SLA	172(7)a	132(7)cd	154(8)b	123(7)d	143(7)b	141(7)bc	136(8)c	112(8)e
N_{area}	1.3(0.1)b	0.8(0.1)d	1.3(0.1)b	0.8(0.1)d	1.9(0.1)a	1.1(0.1)c	1.4(0.1)b	1.1(0.1)c

Within rows, means followed by the same letter do not differ significantly at $\alpha = 0.05$ based on Tukey's test. ANOVA results are given in [S1 Table](#).

<https://doi.org/10.1371/journal.pone.0206021.t002>

V_{cmax} peaked at 33°C and 34°C ([Fig 4; Table 2](#)) and apparent J peaked at 34°C and 30°C ([Fig 4; Table 2](#)) for clones MxB and MxN respectively. However, apparent V_{cmax} and apparent J did not show any deactivation at warm temperature ([Fig 4](#)). The activation energy (E_a) of apparent V_{cmax} and J , decreased with increasing growth temperature for clone MxB and remained constant for clone MxN ([Table 2](#)).

Temperature response of stomatal conductance (g_s)

g_s decreased under all treatments and for both clones when T_{leaf} was increased over the 10–40°C gradient ([Fig 5](#)). g_s at the growth temperature, derived from the g_s - T response curves (g_{s_growth}) was influenced by both clone and growth temperature. For clone MxB, g_{s_growth} was

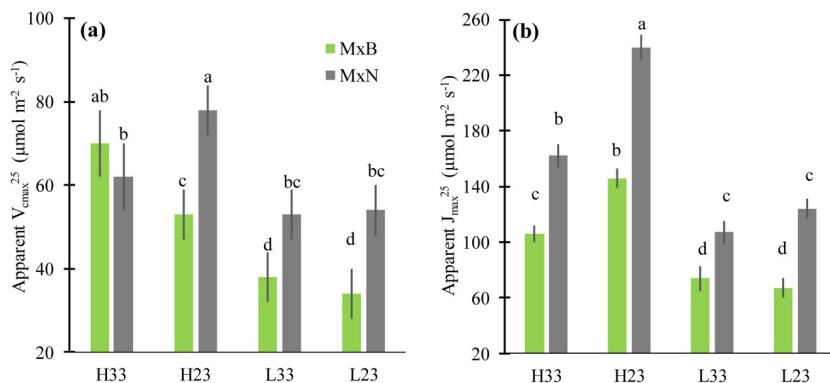


Fig 3. Apparent maximum carboxylation rate of RuBisCO at leaf temperature of 25°C (V_{cmax}^{25}) (a), and apparent maximum electron transport rate at leaf temperature of 25°C (J_{max}^{25}) (b) for two hybrid poplar clones (MxB) and (MxN) grown under two temperatures and two nitrogen levels. See [Fig 2](#) for abbreviation. Data are represented by means \pm SE (n = 3). Means having the same letters are not significantly different at $\alpha = 0.05$ based on Tukey's tests.

<https://doi.org/10.1371/journal.pone.0206021.g003>

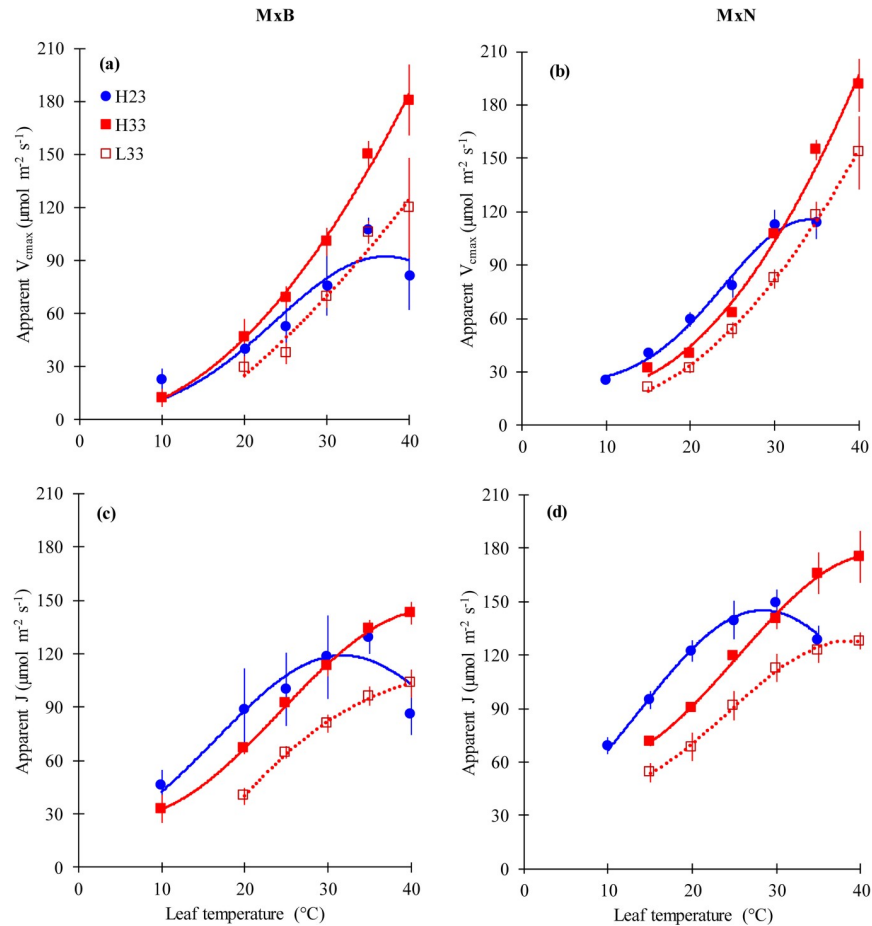


Fig 4. The temperature dependence of the apparent maximum carboxylation capacity of RuBisCO (V_{cmax}) and the apparent electron transport rate (J) for clone MxB (a, c) and clone MxN (b, d) grown under two temperatures and two nitrogen levels. See Fig 2 for symbols. L23 treatment was not given for both clones because A-Ci curves at 35 and 40°C failed to converge and estimates of V_{cmax} and J could not be obtained. Data are represented by means \pm SE ($n = 3$). P value and R^2 of curves are given in S2 Table.

<https://doi.org/10.1371/journal.pone.0206021.g004>

62.5% and 17% higher at warm, compared to cooler growth temperature under high and low nitrogen level respectively (Table 2). Conversely, for clone MxN, g_{s_growth} was similar among growth temperature at high N level averaging $0.19 \text{ mol H}_2\text{O m}^{-2} \text{ s}^{-1}$ and decreased by increasing growth temperature at low N level (0.16 vs. $0.13 \text{ mol H}_2\text{O m}^{-2} \text{ s}^{-1}$).

Specific leaf area and leaf nitrogen

Leaf nitrogen content expressed on an area basis (N_{area}) was increased under high N treatment for both clones. Growth temperature impacted negatively N_{area} of clone MxN only at high N level (Table 2). SLA decreased by increasing growth temperature except for clone MxB under low N. Also, SLA was greater in HN than LN except for clone MxN at 23°C (Table 2).

RuBisCO and RuBisCO activase amount

The relative amount of RuBisCO (RAR) decreased significantly when N level changed from high to low, except for MxN at 23°C (Fig 6A). RAR did not change in response to change of growth temperature for both clones (Fig 6A). In addition, at high N level, RAR was similar

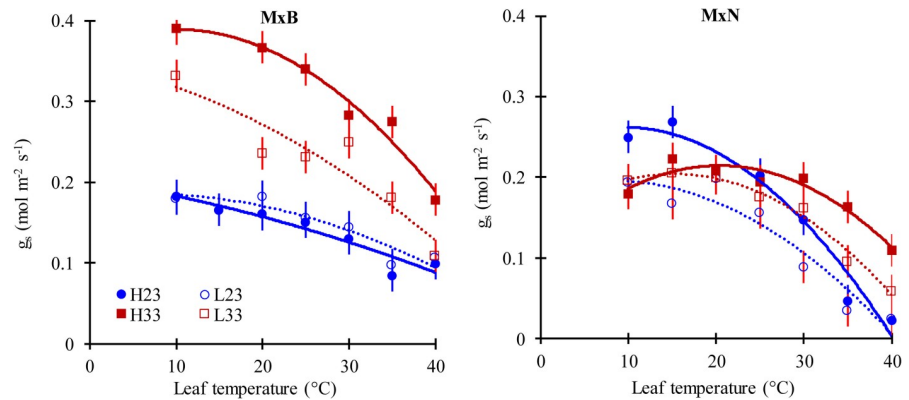


Fig 5. The response of stomatal conductance (g_s) to leaf temperature of two hybrid poplar clones (MxB) and (MxN) grown under two temperatures and two nitrogen levels ($n = 3$). See Fig 2 for symbols. Data are represented by means \pm SE ($n = 3$). P value and R^2 of curves are given in S2 Table.

<https://doi.org/10.1371/journal.pone.0206021.g005>

between clones, being around 0.8 on average. At low N level, RAR was two folds higher for clone MxN compared to clone MxB (Fig 6A). Nitrogen enrichment remarkably increased the relative amount of RuBisCO activase (RARCA), particularly for clone MxN which had a lower RARCA at low N level, compared to MxB (Fig 6B). RARCA was stimulated by warmer growth temperature for MxN at high N and for MxB at low N, but no difference was found for the two other clone-N combinations (Fig 6B). More importantly, the ratio of short isoform to large isoform of RuBisCO activase was markedly stimulated by warm conditions for clone MxN and only at low N for clone MxB (Fig 7).

Discussion

Thermal acclimation of A_n and R_d

The two hybrid poplar clones showed a clear thermal acclimation of A_n by adjusting A_{n-opt} and/or T_{opt} to growth temperature. This is in accordance with results of [33] on cold and

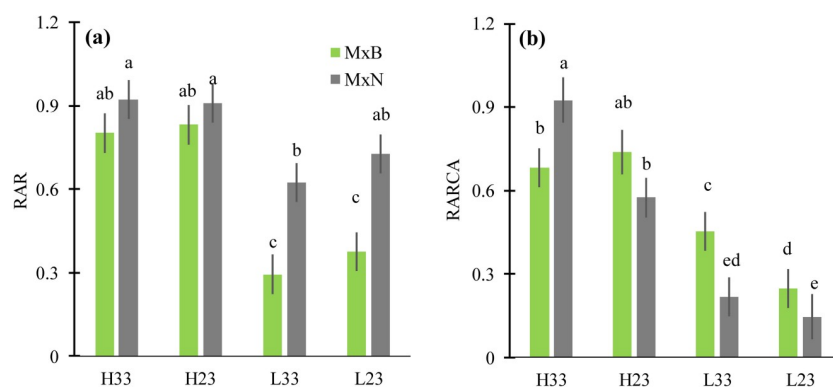


Fig 6. Relative amounts of RuBisCO (RAR) (a) and RuBisCO-activase (RARCA) (b) measured by western blot for two hybrid poplar clones (MxB) and (MxN) grown under two temperatures and two nitrogen levels ($n = 3$). Proteins were extracted from leaves and analyzed by SDS-PAGE. Immunoblots were probed with anti-RuBisCO or anti-RuBisCO activase antibody (S1 Fig). H23 and L23 are treatments of high and low nitrogen level respectively at 23°C ambient daytime temperature; H33 and L33 are treatments of low and high nitrogen level at 33°C ambient daytime temperature. Data are represented by means \pm SD ($n = 3$). Means having the same letters are not significantly different at $\alpha = 0.05$ based on Tukey's tests.

<https://doi.org/10.1371/journal.pone.0206021.g006>

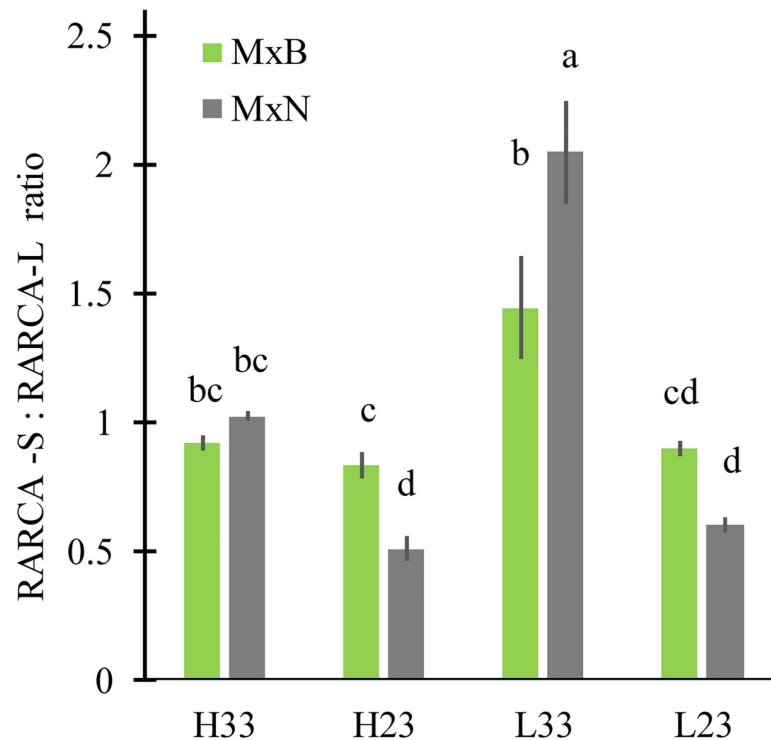


Fig 7. Ratio of short to long isoform of RuBisCO activase of two hybrid poplar grown under two temperatures and two nitrogen levels (n = 3). RCA-S: the short isoform of RuBisCO activase; RCA-L: the long isoform of RuBisCO activase. Data are represented by means ± SE (n = 3). Means having the same letters are not significantly different at $\alpha = 0.05$ based on Tukey's test.

<https://doi.org/10.1371/journal.pone.0206021.g007>

warm ecotypes of *Populus balsamifera* which maintained A_{n-opt} without an evident change of T_{opt} . We found that T_{opt} of A_n under warm temperature was identical to mean growth temperature (the average of day time/night-time = 30°C) and was 3°C below the daytime growth temperature (33°C) suggesting a limited acclimation of photosynthesis rate if we assume the latter was unrelated to night-time temperature. So far, studies focusing on night-time temperature effect on A_n are very scarce [47]. T_{opt} of A_n for clone M×N was lowered by low nitrogen level under warm conditions. The net photosynthetic rates at the growth temperature ($A_{n-growth}$), a relevant quantitative trait that reflects thermal acclimation of A_n [6, 7], was enhanced in plants grown at the warm temperature for clone M×B and remained unchanged for clone M×N. These results suggest a differential thermal adaptation range of the two hybrid poplar clones which could result from the climate of origin of their parents [33]. In a recent meta-analysis, Kumarathunge et al.'s [48] reported that the modulation of T_{opt} and A_{opt} in response to the change in growth temperature was driven by acclimation and, to a lesser extent, by local genetic adaptation to the climate of origin.

Thermal acclimation of R_d is very common for C_3 plants and several studies reported a downshift in the rate of R_d (so-called Type II acclimation) and a decrease of Q_{10} (so-called Type I acclimation) in response to warmer temperatures [49, 50] but few studies on *Populus* exist in this regard [33, 36, 51, 52]. In accordance with the findings of Tjoelker et al.'s [52] for *Populus tremula*, we found substantial Type I and II acclimation of R_d to the growth temperature for clone M×N. In contrast, no acclimation of R_d was observed for clone M×B. The contrasting thermal acclimation capacity observed for the two hybrid poplar clones may be associated to the modulation capacity of the density of mitochondria and the expression of the

alternative oxidative pathway (AOX) [49, 53]. In fact, the increase of growth temperature generally induces a decrease in AOX protein abundance and density of mitochondria [3].

Thermal acclimation of non-photorespiratory mitochondrial respiration in the light (R_{day}) is an important and less investigated component of thermal acclimation of A_n [6]. R_{day} is generally strongly correlated with R_d and assumed to be half R_d [6, 54]. The temperature response of R_{day} and its acclimation to growth temperature has been found to mirror those of R_d for some species [6]. Therefore, we may expect the involvement of R_{day} in the observed acclimation of A_n of our study if we assume a similar response of R_{day} compared to R_d .

Thermal response of photosynthetic biochemical limitations

The effect of growth temperature on temperature response curve of apparent V_{cmax} and J in terms of their values at reference temperature of 25°C, their T_{opt} and their activation energy is species-dependent as reported by recent studies [6, 9, 19, 23, 55, 56]. In our study, the apparent V_{cmax}^{25} stimulated by warm growth temperature for clone M×B, might explain the noticeable increase of A_{n-opt} (up to 50%) by warmer growth conditions under high N level. In parallel, the small decrease in the apparent V_{cmax}^{25} at warm growth conditions observed for clone M×N might explain the observed similar A_{n-opt} under the two growth temperatures. These results are in agreement with the findings of other studies showing a similar or a greater V_{cmax}^{25} when growth temperature increased [6, 33, 56, 57]. In contrast, the apparent J_{max}^{25} decreased at warmer growth temperature as reported for *Populus balsamifera* [33] and other tree species [6, 56, 58].

Hikosaka et al.s [9] suggested an increase in the activation energy of V_{cmax} (E_a) with an increase in growth temperature as an explanatory mechanism of thermal acclimation of A_n (at least by the increase of T_{opt} with growth temperature). Our results are diverging with this postulate since we observed no change in E_a for clone M×N and a remarkable decrease of E_a for clone M×B. However, the patterns we observed have been reported for several species including *Populus tremuloides* [34], *Populus balsamifera* [33] and *Corymbia calophylla* [57].

The temperature optimum (T_{opt}) of apparent V_{cmax} and J acclimated to growth temperature (Fig 4) as observed for other species [17, 23] and may have contributed in the observed acclimation of A_n (Fig 2).

The adjustment of leaf nitrogen invested in soluble vs. insoluble proteins in response to change in growth temperature, inferred from J_{max}^{25} to V_{cmax}^{25} ratio, can be achieved through the maintenance of an optimal balance between the rate of photosynthetic carboxylation vs. RuBP regeneration. This mechanism allows plants to maximize the photosynthetic rate at a given growth temperature [23, 55]. Therefore, the decrease of $J_{max}^{25}:V_{cmax}^{25}$ ratio consequent to an increase of growth temperature has been reported to significantly contribute to thermal acclimation of A_n [17, 23, 48, 56]. In our study, this pattern occurred for clone M×B under high N level which increased both V_{cmax}^{25} and A_{n-opt} . Conversely, the lack of modulation of $J_{max}^{25}:V_{cmax}^{25}$ ratio for clone M×N may have contributed to the observed decrease in V_{cmax}^{25} and to the maintenance of A_{n-opt} . Under low N level, A_{n-opt} of M×B increased under warmer conditions without any change of the $J_{max}^{25}:V_{cmax}^{25}$ ratio. Therefore, the increase of V_{cmax}^{25} and A_{n-opt} under the warm growth temperature cannot be attributed only to the shift in $J_{max}^{25}:V_{cmax}^{25}$ ratio.

Stomatal conductance

The contribution of diffusional limitations to thermal acclimation of A_n remains non-well quantified for several species, including *Populus*. Our results demonstrate that the modulation of g_s (the shape of the relationship between g_s and T_{leaf} and the value of g_s at growth

temperature) in response to changes in growth temperature (Fig 5) may contribute to the observed thermal acclimation of A_n as previously reported [33, 56, 57]. Also, our results suggest that the stomatal acclimation to growth temperature may be clone-specific and may have a significant impact on clone response to warming depending on soil water status. The CO_2 diffusion in the mesophyll shares the same pathways of water transport from mesophyll to the atmosphere [38, 59] and may lead to a similar response of stomatal and mesophyll conductance to growth conditions. Moreover, a link between mesophyll conductance (g_m) and hydraulic conductance has been reported as well [54, 59], suggesting that the observed response of g_s to growth temperature may have originated from modulation of g_m and hydraulic functioning.

RuBisCO and RuBisCO activase amounts in response to experimental warming

The RuBisCO content in our study was quite sensitive to nitrogen level but not to growth temperature. Neither thermal acclimation of A_n (T_{opt} and A_{n-opt}) nor $J_{max}^{25}:V_{cmax}^{25}$ ratio was affected by RuBisCO content. The absence of any effect of RuBisCO content on traits related to thermal acclimation of A_n has also been reported by Weston et al.'s [24] and Kruse et al.'s [60], while other studies found a significant decrease in V_{cmax}^{25} linked to a decrease in RuBisCO and leaf nitrogen content [16, 17]. Thus, the relationship between the change in RuBisCO content in response to growth temperature and thermal acclimation of A_n via the modulation of photosynthetic capacity attributes (V_{cmax}^{25} and J_{max}^{25}) is, most likely, depending on species and environmental parameters (e.g. nitrogen availability). Indeed, CO_2 conductance, R_{day} , the variation of RuBisCO activase content and the temperature dependency of RuBisCO kinetic properties have been reported to be determinant factors of the V_{cmax}^{25} response to growth temperature and consequently thermal acclimation of A_n [6, 20, 45, 61]. The increase of leaf RuBisCO activase amount by increased growth temperature has been reported for several tree species [24, 27–31]. In our study, the hypothesized increase of RARCA at warmer growth temperature was observed only for clone M×N at high N and for clone M×B at low N. Likely, having more than three replicates per treatment ($n = 3$) could make this trend more obvious. Besides, our results demonstrated that the increase of RARCA under warm conditions resulted mainly from increased synthesis of the short isoform suggesting that the two isoforms operate at different temperature optima.

Overall, we think that using a larger set of clones would help assess the adaptive value of thermal acclimation and dissect its genetic control and molecular mechanisms [62]. Also, our study highlighted the complexity of assessing thermal acclimation of photosynthesis as a multi-trait process and the need for further investigation regarding the involvement of mesophyll conductance and hydraulic conductivity as well as the expression of the photosynthesis-related pool of proteins to better understand the mechanistic basis of the observed trends.

In conclusion, the observed thermal acclimation of photosynthesis under our experimental conditions was clearly related to the modulation of photosynthetic capacity and g_s in response to growth temperature. The modulation of the photosynthetic capacity was mainly linked to RuBisCO activase but not RuBisCO content. On the other hand, our results do not support the involvement of leaf N status in thermal acclimation of A_n and R_d .

Supporting information

S1 Fig. Western blot of RuBisCO and RuBisCO activase for two hybrid poplar clones (M×N and M×B) under combinations of growth temperature (23°C and 33°C) and

nitrogen level (high level: HN and low level: LN).
(PDF)

S1 File. ACi curve data.
(TXT)

S1 Table. Analysis of variance, *F* and *P* values for thermal acclimation-related traits.
(PDF)

S2 Table. *P* value and R^2 of curves in Figs 1, 2 and 3.
(PDF)

Acknowledgments

We thank Dr. G Ethier for his valuable comments on A-Ci curve analysis. We also thank F Larochelle and M Coyea (Université Laval) for their technical assistance throughout the project.

Author Contributions

Conceptualization: Lahcen Benomar, Mohamed Taha Moutaoufik, Raed Elferjani, Nathalie Isabel, Annie DesRochers.

Data curation: Lahcen Benomar, Mohamed Taha Moutaoufik.

Formal analysis: Lahcen Benomar, Mohamed Taha Moutaoufik, Raed Elferjani, Rim Khelifa.

Funding acquisition: Nathalie Isabel, Annie DesRochers.

Investigation: Lahcen Benomar, Ahmed El Guellab, Rim Khelifa.

Methodology: Lahcen Benomar, Mohamed Taha Moutaoufik, Raed Elferjani, Ahmed El Guellab, Lala Amina Idrissi Hassania.

Project administration: Lahcen Benomar.

Resources: Lahcen Benomar, Nathalie Isabel.

Software: Lahcen Benomar, Mohamed Taha Moutaoufik.

Supervision: Lahcen Benomar.

Validation: Mohamed Taha Moutaoufik, Lala Amina Idrissi Hassania.

Visualization: Mohamed Taha Moutaoufik.

Writing – original draft: Lahcen Benomar, Raed Elferjani.

Writing – review & editing: Mohamed Taha Moutaoufik, Raed Elferjani, Nathalie Isabel, Annie DesRochers, Ahmed El Guellab, Rim Khelifa, Lala Amina Idrissi Hassania.

References

1. Lloyd J, Farquhar GD. Effects of rising temperatures and [CO₂] on the physiology of tropical forest trees. *Philos Trans R Soc Lond B Biol Sci*. 2008; 363(1498):1811–7. Epub 2008/02/13. <https://doi.org/10.1098/rstb.2007.0032> PMID: 18267901
2. Sage RF, Way DA, Kubien DS. Rubisco, Rubisco activase, and global climate change. *Journal of Experimental Botany*. 2008; 59(7):1581–95. <https://doi.org/10.1093/jxb/ern053> PMID: 18436544
3. Atkin OK, Bruhn D, Tjoelker MG. Response of plant respiration to changes in temperature: Mechanisms and consequences of variations in Q₁₀ values and acclimation. In: Lambers H, Ribas-Carbo M, editors. *Plant Respiration: From Cell to Ecosystem*. Dordrecht: Springer Netherlands; 2005. p. 95–135.

4. Medlyn BE, Dreyer E, Ellsworth D, Forstreuter M, Harley PC, Kirschbaum MUF, et al. Temperature response of parameters of a biochemically based model of photosynthesis. II. A review of experimental data. *Plant, Cell & Environment*. 2002; 25(9):1167–79. <https://doi.org/10.1046/j.1365-3040.2002.00891.x>
5. Sage RF, Kubien DS. The temperature response of C3 and C4 photosynthesis. *Plant Cell and Environment*. 2007; 30(9):1086–106. <https://doi.org/10.1111/j.1365-3040.2007.01682.x> PMID: 17661749
6. Way DA, Yamori W. Thermal acclimation of photosynthesis: on the importance of adjusting our definitions and accounting for thermal acclimation of respiration. *Photosynthesis Research*. 2014; 119(1):89–100. <https://doi.org/10.1007/s11120-013-9873-7> PMID: 23812760
7. Yamori W, Hikosaka K, Way DA. Temperature response of photosynthesis in C3, C4, and CAM plants: temperature acclimation and temperature adaptation. *Photosynthesis Research*. 2014; 119(1–2):101–17. <https://doi.org/10.1007/s11120-013-9874-6> PMID: 23801171
8. Yamori W, Noguchi K, Hikosaka K, Terashima I. Cold-tolerant crop species have greater temperature homeostasis of leaf respiration and photosynthesis than cold-sensitive species. *Plant and Cell Physiology*. 2009; 50(2):203–15. <https://doi.org/10.1093/pcp/pcn189> PMID: 19054809
9. Hikosaka K, Ishikawa K, Borjigidai A, Muller O, Onoda Y. Temperature acclimation of photosynthesis: mechanisms involved in the changes in temperature dependence of photosynthetic rate. *Journal of Experimental Botany*. 2006; 57(2):291–302. <https://doi.org/10.1093/jxb/erj049> PMID: 16364948
10. DesRochers A, Driessche Rvd, Thomas BR. Nitrogen fertilization of trembling aspen seedlings grown on soils of different pH. *Canadian Journal of Forest Research*. 2003; 33(4):552–60. <https://doi.org/10.1139/x02-191>
11. Fisichelli NA, Stefanski A, Frelich LE, Reich PB. Temperature and leaf nitrogen affect performance of plant species at range overlap. *Ecosphere*. 2015; 6(10):1–4. <https://doi.org/10.1890/ES15-00115.1>
12. Field C. Allocating leaf nitrogen for the maximization of carbon gain: Leaf age as a control on the allocation program. *Oecologia*. 1983; 56(2):341–7.
13. Poorter H, Niinemets Ü, Poorter L, Wright IJ, Villar R. Causes and consequences of variation in leaf mass per area (LMA): a meta-analysis. *New Phytologist*. 2009; 182(3):565–88. <https://doi.org/10.1111/j.1469-8137.2009.02830.x> PMID: 19434804
14. Reich PB, Oleksyn J. Global patterns of plant leaf N and P in relation to temperature and latitude. *Proceedings of the National Academy of Sciences of the United States of America*. 2004; 101(30):11001–6. <https://doi.org/10.1073/pnas.0403588101> PMID: 15213326
15. Gunderson CA, O'Hara KH, Campion CM, Walker AV, Edwards NT. Thermal plasticity of photosynthesis: the role of acclimation in forest responses to a warming climate. *Global Change Biology*. 2010; 16(8):2272–86. <https://doi.org/10.1111/j.1365-2486.2009.02090.x>
16. Scafaro AP, Xiang S, Long BM, Bahar NHA, Weerasinghe LK, Creek D, et al. Strong thermal acclimation of photosynthesis in tropical and temperate wet-forest tree species: the importance of altered Rubisco content. *Global Change Biology*. 2017; 23(7): 2783–2800. <https://doi.org/10.1111/gcb.13566> PMID: 27859952
17. Crous KY, Drake JE, Aspinwall MJ, Sharwood RE, Tjoelker MG, Ghannoum O. Photosynthetic capacity and leaf nitrogen decline along a controlled climate gradient in provenances of two widely distributed *Eucalyptus* species. *Global Change Biology*. 2018; 24(10):4626–44. <https://doi.org/10.1111/gcb.14330> PMID: 29804312
18. Yamori W, Nagai T, Makino A. The rate-limiting step for CO₂ assimilation at different temperatures is influenced by the leaf nitrogen content in several C3 crop species. *Plant, Cell & Environment*. 2011; 34(5):764–77. <https://doi.org/10.1111/j.1365-3040.2011.02280.x> PMID: 21241332
19. Benomar L, Lamhamedi MS, Pepin S, Rainville A, Lambert MC, Margolis HA, et al. Thermal acclimation of photosynthesis and respiration of southern and northern white spruce seed sources tested along a regional climatic gradient indicates limited potential to cope with temperature warming. *Ann Bot*. 2018; 121(3):443–57. Epub 2018/01/05. <https://doi.org/10.1093/aob/mcx174> PMID: 29300870
20. Qiu C, Ethier G, Pepin S, Dubé P, Desjardins Y, Gosselin A. Persistent negative temperature response of mesophyll conductance in red raspberry (*Rubus idaeus* L.) leaves under both high and low vapour pressure deficits: a role for abscisic acid? *Plant, Cell & Environment*. 2017; 40(9):1940–59. <https://doi.org/10.1111/pce.12997> PMID: 28620951
21. Warren CR. Does growth temperature affect the temperature responses of photosynthesis and internal conductance to CO₂? A test with *Eucalyptus regnans*. *Tree Physiol*. 2008; 28(1):11–9. Epub 2007/10/17. PMID: 17938109
22. von Caemmerer S, Evans JR. Temperature responses of mesophyll conductance differ greatly between species. *Plant Cell and Environment*. 2015; 38(4):629–37. <https://doi.org/10.1111/pce.12449> PMID: 25224884

23. Kattge J, Knorr W. Temperature acclimation in a biochemical model of photosynthesis: a reanalysis of data from 36 species. *Plant, Cell & Environment*. 2007; 30(9):1176–90. <https://doi.org/10.1111/j.1365-3040.2007.01690.x> PMID: 17661754
24. Weston DJ, Bauerle WL, Swire-Clark GA, Moore Bd, Baird WV. Characterization of Rubisco activase from thermally contrasting genotypes of *Acer rubrum* (Aceraceae). *American Journal of Botany*. 2007; 94(6):926–34. <https://doi.org/10.3732/ajb.94.6.926> PMID: 21636461
25. Cen Y-P, Sage RF. The regulation of rubisco activity in response to variation in temperature and atmospheric CO₂ partial pressure in sweet potato. *Plant Physiology*. 2005; 139(2):979–90. <https://doi.org/10.1104/pp.105.066233> PMID: 16183840
26. Salvucci ME, Crafts-Brandner SJ. Relationship between the Heat Tolerance of Photosynthesis and the Thermal Stability of Rubisco Activase in Plants from Contrasting Thermal Environments. *Plant Physiology*. 2004; 134(4):1460–70. <https://doi.org/10.1104/pp.103.038323> PMID: 15084731
27. Crafts-Brandner SJ, Salvucci ME. Rubisco activase constrains the photosynthetic potential of leaves at high temperature and CO₂. *Proceedings of the National Academy of Sciences*. 2000; 97(24):13430–5. <https://doi.org/10.1073/pnas.230451497> PMID: 11069297
28. Yamori W, von Caemmerer S. Effect of rubisco activase deficiency on the temperature response of CO₂ assimilation rate and rubisco activation state: Insights from transgenic tobacco with reduced amounts of rubisco activase. *Plant Physiology*. 2009; 151(4):2073–82. <https://doi.org/10.1104/pp.109.146514> PMID: 19837817
29. Hozain Mdl Salvucci ME, Fokar M Holaday AS. The differential response of photosynthesis to high temperature for a boreal and temperate *Populus* species relates to differences in Rubisco activation and Rubisco activase properties. *Tree Physiology*. 2009; 30(1):32–44. <https://doi.org/10.1093/treephys/tpp091> PMID: 19864261
30. Law DR, Crafts-Brandner SJ, Salvucci ME. Heat stress induces the synthesis of a new form of ribulose-1,5-bisphosphate carboxylase/oxygenase activase in cotton leaves. *Planta*. 2001; 214(1):117–25. <https://doi.org/10.1007/s004250100592> PMID: 11762161
31. Ristic Z, Momčilović I, Bukovnik U, Prasad PVV, Fu J, DeRidder BP, et al. Rubisco activase and wheat productivity under heat-stress conditions. *Journal of Experimental Botany*. 2009; 60(14):4003–14. <https://doi.org/10.1093/jxb/erp241> PMID: 19671572
32. Wang D, Li X-F, Zhou Z-J, Feng X-P, Yang W-J, Jiang D-A. Two Rubisco activase isoforms may play different roles in photosynthetic heat acclimation in the rice plant. *Physiologia Plantarum*. 2010; 139(1):55–67. <https://doi.org/10.1111/j.1399-3054.2009.01344.x> PMID: 20059735
33. Silim S, Ryan N, Kubien D. Temperature responses of photosynthesis and respiration in *Populus balsamifera* L.: acclimation versus adaptation. *Photosynthesis Research*. 2010; 104(1):19–30. <https://doi.org/10.1007/s11120-010-9527-y> PMID: 20112068
34. Dillaway DN, Kruger EL. Thermal acclimation of photosynthesis: a comparison of boreal and temperate tree species along a latitudinal transect. *Plant Cell and Environment*. 2010; 33(6):888–99. <https://doi.org/10.1111/j.1365-3040.2010.02114.x> PMID: 20082671
35. Centritto M, Brillì F, Fodale R, Loreto F. Different sensitivity of isoprene emission, respiration and photosynthesis to high growth temperature coupled with drought stress in black poplar (*Populus nigra*) saplings. *Tree Physiology*. 2011; 31(3):275–86. <https://doi.org/10.1093/treephys/tpq112> PMID: 21367745
36. Ow LF, Griffin KL, Whitehead D, Walcroft AS, Turnbull MH. Thermal acclimation of leaf respiration but not photosynthesis in *Populus deltoides* x *nigra*. *New Phytologist*. 2008; 178(1):123–34. <https://doi.org/10.1111/j.1469-8137.2007.02357.x> PMID: 18221247
37. Farquhar GD, von Caemmerer S, Berry JA. A biochemical model of photosynthetic CO₂ assimilation in leaves of C₃ species. *Planta*. 1980; 149(1):78–90. <https://doi.org/10.1007/BF00386231> PMID: 24306196
38. Ethier GJ, Livingston NJ. On the need to incorporate sensitivity to CO₂ transfer conductance into the Farquhar–von Caemmerer–Berry leaf photosynthesis model. *Plant Cell and Environment*. 2004; 27(2):137–53. <https://doi.org/10.1111/j.1365-3040.2004.01140.x>
39. Miao Z, Xu M, Lathrop RG Jr., Wang Y. Comparison of the A-Cc curve fitting methods in determining maximum ribulose 1.5-bisphosphate carboxylase/oxygenase carboxylation rate, potential light saturated electron transport rate and leaf dark respiration. *Plant Cell and Environment*. 2009; 32(2):109–22. Epub 2009/01/22. <https://doi.org/10.1111/j.1365-3040.2008.01900.x> PMID: 19154228
40. Dubois JJ, Fiscus EL, Booker FL, Flowers MD, Reid CD. Optimizing the statistical estimation of the parameters of the Farquhar–von Caemmerer–Berry model of photosynthesis. *New Phytol*. 2007; 176(2):402–14. Epub 2007/09/25. <https://doi.org/10.1111/j.1469-8137.2007.02182.x> PMID: 17888119
41. Bernacchi CJ, Singaas EL, Pimentel C, Portis AR Jr, Long SP. Improved temperature response functions for models of Rubisco-limited photosynthesis. *Plant, Cell & Environment*. 2001; 24(2):253–9. <https://doi.org/10.1111/j.1365-3040.2001.00668.x>

42. Battaglia M, Beadle C, Loughhead S. Photosynthetic temperature responses of *Eucalyptus globulus* and *Eucalyptus nitens*. *Tree Physiology*. 1996; 16(1–2):81–9. <https://doi.org/10.1093/treephys/16.1–2.81> PMID: 14871750
43. Bradford MM. A rapid and sensitive method for the quantitation of microgram quantities of protein utilizing the principle of protein-dye binding. *Analytical Biochemistry*. 1976; 72(1):248–54. [https://doi.org/10.1016/0003-2697\(76\)90527-3](https://doi.org/10.1016/0003-2697(76)90527-3)
44. Rasband WS. ImageJ, U. S. National Institutes of Health, Bethesda, Maryland, USA. 2016.
45. Perdomo JA, Capó-Bauçà S, Carmo-Silva E, Galmés J. Rubisco and Rubisco activase play an important role in the biochemical limitations of photosynthesis in rice, wheat, and maize under high temperature and water deficit. *Frontiers in Plant Science*. 2017; 8(490). <https://doi.org/10.3389/fpls.2017.00490> PMID: 28450871
46. Prins A, van Heerden PDR, Olmos E, Kunert KJ, Foyer CH. Cysteine proteinases regulate chloroplast protein content and composition in tobacco leaves: a model for dynamic interactions with ribulose-1,5-bisphosphate carboxylase/oxygenase (Rubisco) vesicular bodies. *Journal of Experimental Botany*. 2008; 59(7):1935–50. <https://doi.org/10.1093/jxb/ern086> PMID: 18503045
47. Turnbull M H, Murthy R, L GK. The relative impacts of daytime and night-time warming on photosynthetic capacity in *Populus deltoides*. *Plant, Cell & Environment*. 2002; 25(12):1729–37. <https://doi.org/10.1046/j.1365-3040.2002.00947.x>
48. Kumarathunge DP, Medlyn BE, Drake JE, Tjoelker MG, Aspinwall MJ, Battaglia M, et al. Acclimation and adaptation components of the temperature dependence of plant photosynthesis at the global scale. *New Phytologist*. 2019. <https://doi.org/10.1111/nph.15668> PMID: 30597597
49. Atkin OK, Tjoelker MG. Thermal acclimation and the dynamic response of plant respiration to temperature. *Trends in Plant Science*. 2003; 8(7):343–51. [https://doi.org/10.1016/S1360-1385\(03\)00136-5](https://doi.org/10.1016/S1360-1385(03)00136-5) PMID: 12878019
50. Reich PB, Sendall KM, Stefanski A, Wei XR, Rich RL, Montgomery RA. Boreal and temperate trees show strong acclimation of respiration to warming. *Nature*. 2016; 531(7596):633–636. <https://doi.org/10.1038/nature17142> PMID: 26982730
51. Dillaway DN, Kruger EL. Leaf respiratory acclimation to climate: comparisons among boreal and temperate tree species along a latitudinal transect. *Tree Physiology*. 2011; 31(10):1114–27. <https://doi.org/10.1093/treephys/tpr097> PMID: 21990024
52. Tjoelker MG, Reich PB, Oleksyn J. Changes in leaf nitrogen and carbohydrates underlie temperature and CO₂ acclimation of dark respiration in five boreal tree species. *Plant, Cell & Environment*. 1999; 22(7):767–78. <https://doi.org/10.1046/j.1365-3040.1999.00435.x>
53. Campbell C, Atkinson L, Zaragoza-Castells J, Lundmark M, Atkin O, Hurry V. Acclimation of photosynthesis and respiration is asynchronous in response to changes in temperature regardless of plant functional group. *New Phytologist*. 2007; 176(2):375–89. <https://doi.org/10.1111/j.1469-8137.2007.02183.x> PMID: 17692077
54. Thérroux-Rancourt G, Éthier G, Pepin S. Threshold response of mesophyll CO₂ conductance to leaf hydraulics in highly transpiring hybrid poplar clones exposed to soil drying. *Journal of Experimental Botany*. 2014; 65(2):741–53. <https://doi.org/10.1093/jxb/ert436> PMID: 24368507
55. Hikosaka K, Murakami A, Hirose T. Balancing carboxylation and regeneration of ribulose-1,5-bisphosphate in leaf photosynthesis: temperature acclimation of an evergreen tree, *Quercus myrsinaefolia*. *Plant Cell and Environment*. 1999; 22(7):841–9. <https://doi.org/10.1046/j.1365-3040.1999.00442.x>
56. Slot M, Winter K. Photosynthetic acclimation to warming in tropical forest tree seedlings. *Journal of Experimental Botany*. 2017; 68(9):2275–84. <https://doi.org/10.1093/jxb/erx071> PMID: 28453647
57. Aspinwall MJ, Vårhammar A, Blackman CJ, Tjoelker MG, Ahrens C, Byrne M, et al. Adaptation and acclimation both influence photosynthetic and respiratory temperature responses in *Corymbia calophylla*. *Tree Physiology*. 2017; 37(8):1095–112. <https://doi.org/10.1093/treephys/tpx047> PMID: 28460131
58. Yamori W, Noguchi K, Kashino Y, Terashima I. The role of electron transport in determining the temperature dependence of the photosynthetic rate in spinach leaves grown at contrasting temperatures. *Plant and Cell Physiology*. 2008; 49(4):583–91. <https://doi.org/10.1093/pcp/pcn030> PMID: 18296450
59. Flexas J, Scoffoni C, Gago J, Sack L. Leaf mesophyll conductance and leaf hydraulic conductance: an introduction to their measurement and coordination. *Journal of Experimental Botany*. 2013; 64(13):3965–81. <https://doi.org/10.1093/jxb/ert319> PMID: 24123453
60. Kruse J, Adams MA, Kadinov G, Arab L, Kreuzwieser J, Alfarraj S, et al. Characterization of photosynthetic acclimation in *Phoenix dactylifera* by a modified Arrhenius equation originally developed for leaf respiration. *Trees*. 2017; 31(2):623–44. <https://doi.org/10.1007/s00468-016-1496-0>

61. Yamori W, Suzuki K, Noguchi K, Nakai M, Terashima I. Effects of Rubisco kinetics and Rubisco activation state on the temperature dependence of the photosynthetic rate in spinach leaves from contrasting growth temperatures. *Plant Cell and Environment*. 2006; 29(8):1659–70. Epub 2006/08/11.
62. Laitinen RAE, Nikoloski Z. Genetic basis of plasticity in plants. *Journal of Experimental Botany*. 2018. <https://doi.org/10.1093/jxb/ery404> PMID: 30445526